

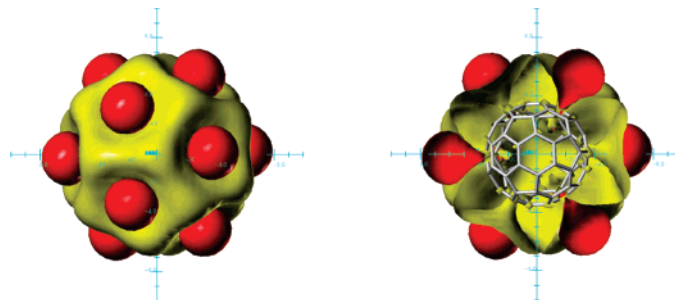
Endohedral and External Through-Space Shieldings of the Fullerenes C₅₀, C₆₀, C₆₀⁻⁶, C₇₀, and C₇₀⁻⁶—Visualization of (Anti)Aromaticity and Their Effects on the Chemical Shifts of Encapsulated Nuclei

Erich Kleinpeter,* Sabrina Klod, and Andreas Koch

Chemisches Institut, Universität Potsdam, P.O. Box 60 15 53, D-14415 Potsdam, Germany

kp@chem.uni-potsdam.de

Received October 26, 2007



Endohedral and external *through-space NMR shieldings* (TSNMRS) and the magnetic susceptibilities of the fullerene carbon cages of C₅₀, C₆₀, C₆₀⁻⁶, C₇₀, and C₇₀⁻⁶ were assessed by ab initio molecular orbital calculations. Employing the *nucleus-independent chemical shift* (NICS) concept, these TSNMRS were visualized as *isochemical shielding surfaces* (ICSS) and were applied to quantitatively estimate either the aromaticity or the anti-aromaticity on the fullerene surface pertaining to the five- or six-membered ring moieties and the shielding of any nuclei enclosed within the carbon cages. Differences between the NICSs calculated at the center of the fullerene carbon cages and the experimental chemical shifts of encapsulated NMR-active nuclei as well as experimental shieldings observed for different encapsulated nuclei were able to be understood readily for the first time.

Introduction

Since the original discovery of fullerenes, the NMR chemical shifts of nuclei inside and outside the carbon sphere have proven to be very interesting for characterizing these compounds with respect to either the aromaticity or anti-aromaticity present. For example, noble gas atoms can be inserted into the cages of the fullerene molecules to form stable compounds. ³He, for instance, is an excellent NMR nucleus and yields, even when encapsulated, well-resolved NMR spectra, thereby reflecting the interior magnetic fields of the carbon cages. Numerous NMR studies of encapsulated noble gases such as ³He@C₆₀,¹ ³He₂@C₇₀,² ³He@C₇₀,^{1c} ³He@C₆₀⁻⁶,^{1e} ³He@C₇₀⁻⁶,^{1ad} ³He₂@C₆₀^{-6,3} ³He₂@C₇₀^{-6,3} endohedral metallofullerenes (e.g., Sc₃N@C₈₀⁴), ¹²⁹Xe@C₆₀,⁵ and open-cage fullerene derivatives^{6,7} (e.g., H₂@C₆₀⁸ and H₂O@C₆₀^{8,9}) have been published with the ensuing trend: ³He and other magnetically active nuclei encapsulated into the fullerene cavity are all strongly shielded. These nuclei have proven to be powerful tools to probe the interior magnetic fields

of the fullerene cages, and in addition, ³He NMR^{10,11} has proven to be a powerful method to follow the chemical transformations of fullerenes.^{1b,c,5,10–13}

(1) (a) Saunders, M.; Jimenez-Vazquez, H. A.; Cross, R. J.; Mroczkowski, S.; Freedberg, D. L.; Anet, F. A. L. *Nature* **1994**, *367*, 256. (b) Saunders, M.; Jimenez-Vazquez, H. A.; Bangerter, B. W.; Cross, R. J.; Mroczkowski, S.; Freedberg, D. I.; Anet, F. A. L. *J. Am. Chem. Soc.* **1994**, *116*, 3621. (c) Saunders, M.; Jimenez-Vazquez, H. A.; Cross, R. J.; Billups, W. E.; Gesenberg, C.; Gonzalez, A.; Luo, W.; Haddon, R. C.; Diederich, F.; Herrmann, A. *J. Am. Chem. Soc.* **1995**, *117*, 9305. (d) Saunders, M.; Cross, R. J.; Jimenez-Vazquez, H. A.; Shimshi, R.; Khong, A. *Science* **1996**, *271*, 1693. (e) Shabtai, E.; Weitz, A.; Haddon, R. C.; Hoffman, R. E.; Rabinovitz, M.; Khong, A.; Cross, R. J.; Saunders, M.; Cheng, P. C.; Scott, L. T. *J. Am. Chem. Soc.* **1998**, *120*, 6389. (f) Wang, G.-W.; Saunders, M.; Khong, A.; Cross, R. J. *J. Am. Chem. Soc.* **2000**, *122*, 3216.

(2) Khong, A.; Jimenez-Vazquez, H. A.; Saunders, M.; Cross, R. J.; Laskin, J.; Peres, T.; Lifshitz, C.; Strongin, R.; Smith, A. B., III. *J. Am. Chem. Soc.* **1998**, *120*, 6380.

(3) Sternfeld, T.; Hoffman, R. E.; Saunders, M.; Cross, R. J.; Syamala, M. S.; Rabinovitz, M. *J. Am. Chem. Soc.* **2002**, *124*, 8786.

(4) Cardona, C. M.; Kitaygorodskiy, A.; Ortiz, A.; Herranz, M. A.; Echegoyen, L. *J. Org. Chem.* **2005**, *70*, 5092.

Theoretical calculations of the endohedral magnetic shielding in fullerenes have been performed¹⁴ at various levels of theory, wherein the ³He chemical shifts in He@C₆₀ and He@C₇₀,¹⁵ as well as in smaller¹⁶ and larger fullerenes,^{16,17} were all reasonably well-reproduced. The calculated endohedral shieldings, as well as the experimental chemical shifts, proved to be reliable probes for the ring current effects active in the fullerenes and were thus able to be used as a criterion of aromaticity.¹⁸ Furthermore, the chemical shifts at the middle points of the pentagons and hexagons and at certain endohedral positions in the fullerene cages (termed *nucleus-independent chemical shift*, NICS)¹⁹ were calculated and have proven to be useful as an interpretative tool for identifying local (anti)aromatic regions.²⁰ The large negative NICSs found at the center of the fullerenes were, to a large extent, attributed to the ring currents of the individual five- and six-membered rings.²⁰

As probes for the external (anti)aromaticity of fullerenes, the proton chemical shifts of methylene protons in bridged fullerenes have been employed.^{4,21} Characteristic differences were obtained depending on the position of the protons, situated above either a five- or a six-membered ring. For two protons located above separate six-membered rings, a chemical shift difference does not arise. However, if one is located above a five-membered ring, moderate to strong chemical shift differences are evi-

dent.^{4,21} Thus, these methylene bridge protons serve as sensors of the local (anti)aromaticity above each ring²² that arises from the paramagnetic/diamagnetic ring currents on the surfaces of the fullerenes.⁴ On this basis, the local aromaticity of certain fullerenes and of their hexa-anions has been estimated.²²

After the introduction of the NICS concept,²⁵ grids of NICS values surrounding various molecules have been assembled to provide insight into the diatropic and paratropic regions of molecules.²³ At about the same time, we visualized²⁴ the *through-space NMR shieldings* (TSNMRS) of double bonds, triple bonds, and analogous heterocyclic functional groups as well as of benzene by *isochemical shielding surfaces* (ICSS) which are easily constructed employing the NICS concept. In this approach, a lattice of “ghost atoms” surrounding the π -electron system located in the center of a virtual cube (10 × 10 × 10 Å) is ab initio MO calculated employing the GIAO perturbation method^{26,27} and the resulting data set transformed into a contour file of ICSS using SYBYL as modeling software.²⁸ It is thus possible to visualize the TSNMRS using ICSS of different intensity by this procedure, and because the NICSs of all the ghost atoms in the data matrix are known, the TSNMRS of the functional group/aromatic moiety can be specified and employed to determine the stereochemistry of any proximal nuclei.^{24,29–43} This approach allowed the re-appraisal of some prevalent assertions in prescribed NMR textbooks. For example, the ¹H chemical shift difference between the *axial* and *equatorial* protons in cyclohexane was not found to be due to the anisotropy of the C–C single bond,³² and the deshielding by 1.57 ppm of H-4 in 11-ethynylphenanthrene relative to its counterpart in phenanthrene was not found to be due to the anisotropy of the C≡C triple bond.³⁷

Similar approaches to estimate TSNMRS have been published by Alkorta and Elguero,⁴⁴ and Martin et al.⁴⁵ In both cases,

(5) Syamala, M. S.; Cross, R. J.; Saunders, M. *J. Am. Chem. Soc.* **2002**, *124*, 6216.

(6) Rubin, Y.; Jarrosson, T.; Wang, G.-W.; Bartberger, M. D.; Houk, K. N.; Schick, G.; Saunders, M.; Cross, R. *J. Angew. Chem., Int. Ed.* **2001**, *40*, 1543.

(7) Nierengarten, J.-F. *Angew. Chem., Int. Ed.* **2001**, *40*, 2973.

(8) Murata, Y.; Murata, M.; Komatsu, K. *J. Am. Chem. Soc.* **2003**, *125*, 7152.

(9) Iwamatsu, S.-I.; Uozaki, T.; Kobayashi, K.; Re, S.; Nagase, S.; Murata, S. *J. Am. Chem. Soc.* **2004**, *126*, 2668 and references cited therein.

(10) Rüttimann, M.; Haldimann, R. F.; Isaacs, L.; Diederich, F.; Khong, A.; Jimenez-Vazquez, H.; Cross, R. J.; Saunders, M. *Chem.—Eur. J.* **1997**, *3*, 1071.

(11) Smith, A. B., III; Strongin, R. M.; Brard, L.; Romanow, W. J. *J. Am. Chem. Soc.* **1994**, *116*, 10831.

(12) Wang, G.-W.; Saunders, M.; Cross, R. J. *J. Am. Chem. Soc.* **2001**, *123*, 256.

(13) Wang, G.-W.; Weedon, B. R.; Meier, M. S.; Saunders, M.; Cross, R. *J. Org. Lett.* **2000**, *2*, 2241.

(14) (a) Cioslowski, J. *J. Am. Chem. Soc.* **1994**, *116*, 3619. (b) Cioslowski, J. *Chem. Phys. Lett.* **1994**, *227*, 361.

(15) Bühl, M.; Thiel, W.; Jiao, H.; Schleyer, P. v. R.; Saunders, M.; Anet, F. A. L. *J. Am. Chem. Soc.* **1994**, *116*, 6005.

(16) (a) Bühl, M.; Thiel, W. *Chem. Phys. Lett.* **1995**, *233*, 585. (b) Chen, Z.; Jiao, H.; Bühl, M.; Hirsch, A.; Thiel, W. *Theor. Chem. Acc.* **2001**, *106*, 352.

(17) Bühl, M.; van Wüllen, C. *Chem. Phys. Lett.* **1995**, *247*, 63.

(18) Bühl, M.; Hirsch, A. *Chem. Rev.* **2001**, *101*, 1153.

(19) Schleyer, P. v. R.; Maerker, C.; Dransfeld, A.; Jiao, H.; Hommes, N. J. R. v. E. *J. Am. Chem. Soc.* **1996**, *118*, 6317.

(20) Bühl, M. *Chem.—Eur. J.* **1998**, *4*, 734.

(21) (a) Suzuki, T.; Li, Q. C.; Khemani, K. C.; Wudl, F. *J. Am. Chem. Soc.* **1992**, *114*, 7301. (b) Smith, A. B., III; Strongin, R. M.; Brard, L.; Furst, G. T.; Romanow, W. J.; Owens, K. G.; King, R. C. *J. Am. Chem. Soc.* **1993**, *115*, 5829. (c) Maggini, M.; Scorrano, G.; Prato, M. *J. Am. Chem. Soc.* **1993**, *115*, 9798. (d) Prato, M.; Suzuki, T.; Wudl, F.; Lucchini, V.; Maggini, M. *J. Am. Chem. Soc.* **1993**, *115*, 7876. (e) Isaacs, L.; Wehrsig, A.; Diederich, F. *Helv. Chim. Acta* **1993**, *76*, 1231. (f) Wilson, S. R.; Lu, Q. *J. Org. Chem.* **1995**, *60*, 6496. (g) Smith, A. B., III; Strongin, R. M.; Brard, L.; Furst, G. T.; Romanow, W. J.; Owens, K. G.; Goldschmidt, R. J.; King, R. C. *J. Am. Chem. Soc.* **1993**, *115*, 5492. (h) Sternfeld, T.; Wudl, F.; Hummelen, K.; Weitz, A.; Haddon, R. C.; Rabinovitz, M. *Chem. Commun.* **1999**, 2411. (i) Kiely, A. F.; Haddon, R. C.; Meier, M. S.; Selegue, J. P.; Brock, C. P.; Patrick, B. O.; Wang, G.-W.; Chen, G.-W. *J. Am. Chem. Soc.* **1999**, *121*, 7971. (j) Sternfeld, T.; Hoffman, R. E.; Thilgen, C.; Diederich, F.; Rabinovitz, M. *J. Am. Chem. Soc.* **2000**, *122*, 9038. (k) Sternfeld, T.; Thilgen, C.; Hoffman, R. E.; Heras, M. d. R. C.; Diederich, F.; Wudl, F.; Scott, L. T.; Mack, J.; Rabinovitz, M. *J. Am. Chem. Soc.* **2002**, *124*, 5734.

(22) Chen, Z.; King, R. B. *Chem. Rev.* **2005**, *105*, 3613.

(23) Schleyer, P. v. R.; Manoharan, M.; Wang, Z. X.; Kiran, B.; Jiao, Y.; Puchta, R.; Hommes, N. J. R. v. E. *Org. Lett.* **2001**, *3*, 2465.

(24) Klod, S.; Kleinpeter, E. *J. Chem. Soc., Perkin Trans. 2* **2001**, 1893.

(25) Chen, Z.; Wannere, C. S.; Corminboeuf, C.; Puchta, R.; Schleyer, P. v. R. *Chem. Rev.* **2005**, *105*, 3842.

(26) Ditchfield, J. R. *Mol. Phys.* **1974**, *27*, 789.

(27) Cheeseman, J. R.; Trucks, G. W.; Keith, T. A.; Frisch, M. J. *J. Chem. Phys.* **1996**, *104*, 5497.

(28) SYBYL 7.1; Tripos Inc., St. Louis MO 63144, 2005.

(29) Toth, G.; Kovacs, J.; Levai, A.; Kleinpeter, E.; Koch, A. *Magn. Reson. Chem.* **2001**, *39*, 251.

(30) Kleinpeter, E.; Holzberger, A. *Tetrahedron* **2001**, *57*, 6941.

(31) Germer, A.; Klod, S.; Peter, M. G.; Kleinpeter, E. *J. Mol. Model.* **2002**, *8*, 231.

(32) Klod, S.; Koch, A.; Kleinpeter, E. *J. Chem. Soc., Perkin Trans. 2* **2002**, 1506.

(33) Kovacs, J.; Toth, G.; Simon, A.; Levai, A.; Koch, A.; Kleinpeter, E. *Magn. Reson. Chem.* **2003**, *41*, 193.

(34) Szatmári, I.; Martinek, T. A.; Lazar, L.; Koch, A.; Kleinpeter, E.; Fülöp, F. *Ann. West Univ. Timisoara, Series Chemistry* **2003**, *12*, 175.

(35) Kleinpeter, E.; Klod, S.; Rudorf, W.-D. *J. Org. Chem.* **2004**, *69*, 4317.

(36) Miklos, F.; Kanizsai, I.; Thomas, S.; Kleinpeter, E.; Sillanpää, R.; Stájer, G. *Heterocycles* **2004**, *63*, 63.

(37) Kleinpeter, E.; Klod, S. *J. Am. Chem. Soc.* **2004**, *126*, 2231.

(38) Szatmári, I.; Martinek, T. A.; Lazar, L.; Koch, A.; Kleinpeter, E.; Neuvonen, K.; Fülöp, F. *J. Org. Chem.* **2004**, *69*, 3645.

(39) Kleinpeter, E.; Klod, S. *J. Mol. Struct.* **2004**, *704*, 79.

(40) Hausmann, J.; Käss, S.; Klod, S.; Kleinpeter, E. *Eur. J. Inorg. Chem.* **2004**, 4402.

(41) Ryppa, C.; Senge, M. O.; Hatscher, S. S.; Kleinpeter, E.; Wacker, P.; Schilde, U.; Wiehe, A. *Chem.—Eur. J.* **2005**, *11*, 3427.

(42) Kleinpeter, E.; Schulenburg, A.; Zug, I.; Hartmann, H. *J. Org. Chem.* **2005**, *70*, 6592.

(43) Kleinpeter, E.; Schulenburg, A. *J. Org. Chem.* **2006**, *71*, 3869.

(44) Alkorta, I.; Elguero, J. *New J. Chem.* **1998**, 381.

shieldings of similar size and direction, comparable with the results of our model and the classical model of Bovey and Johnson⁴⁶ and Haigh and Mallion,^{47,48} were obtained.

Our approach²⁴ provided us with a new method to quantitatively ab initio MO calculate both the through-space effects of certain bonds, of functional groups, and of aromatic moieties on proximal nuclei. In addition, ICSS values of ± 0.1 ppm for *in-plane* and *perpendicular-to-center* perspectives for a large variety of aromatic and anti-aromatic compounds have been utilized as a simple means to compare and quantify their aromatic nature.⁴⁹ The major aim of this paper is to apply the method to the fullerenes C₅₀, C₆₀, C₆₀⁻⁶, C₇₀, and C₇₀⁻⁶ in order to visualize their endohedral and external through-space shieldings and to employ the corresponding ICSS values for a quantitative evaluation of the proton chemical shifts of the methylene protons in bridged fullerenes.

Results and Discussion

Endohedral TSNMRS. The grids of TSNMRS within the fullerenes obtained by our approach outlined above were analyzed with respect to the aromaticity of these molecules and visualized as ICSS (see Figure 1). The NICS values at the center of the fullerenes, together with calculated and experimental chemical shifts, are given in Table 1. Also included are the published chemical shifts of a number of endohedrally positioned, magnetically active nuclei encapsulated either in open-cage fullerenes or in derivatives of C₆₀ and C₇₀; the results are of similar sign (i.e., either shielding or deshielding) and magnitude.^{6–13}

The interior magnetic fields of the fullerene cavities are deemed to be very homogeneous for the bulk of the cavity, at least until the walls are reached,^{18,22} as concluded from the identical ³He chemical shifts for ³He@C₇₀ and ³He₂@C₇₀.^{2,3} In Figure 1, various endohedral ICSS values for the fullerenes C₅₀, C₆₀, and C₇₀ are depicted. The TSNMRS at the centers of C₅₀ (−10.7 ppm), C₆₀ (−11.3 ppm), C₆₀⁻⁶ (−64 ppm), C₇₀ (−25.9 ppm), and C₇₀⁻⁶ (−10.6 ppm) are very close to the literature values (cf. Table 1) and to the magnetic susceptibilities of the fullerenes studied (cf. Table 2). However, the ICSSs form

channels of different sign starting from the cage center either through the six-membered ring middle points (generally shielding) or through the five-membered ring ones (deshielding except in the case of the *apical* pentagons in C₅₀ where they are shielding, vide infra). Thus, the TSNMRS in the cavity of the carbon cages are not homogeneous, rather heterogeneous, as can be readily seen in Figure 1. Only near the center are the shielding effects radially consistent. The same result was obtained by following the NICS values on direct lines from the cage center to the middle points of the five-membered or six-membered ring moieties of C₆₀, C₇₀, and both their anions.²² Thus, TSNMRS and hence the chemical shifts of encapsulated magnetically active nuclei are dependent on their position in the cavity. This result concurs with experimental observations: the small size of He atoms or H₂ molecules encapsulated in C₆₀ allows them to be located anywhere in the bulk of the cavity positioned [$\Delta\delta(^3\text{He}) = -6.0$ ppm;^{1a} $\Delta\delta(^1\text{H}_2) = -5.41$ ppm]⁶ but the larger Xe atoms or H₂O molecules are forced to the center of the fullerene cages, and therefore, they experience greater shielding [$\Delta\delta(^{129}\text{Xe}) = -8.89$ ppm;⁵ $\Delta\delta(^1\text{H}_2\text{O}) = -11.40$ ppm].⁹ These values are very near to the calculated^{15,20} chemical shifts of the encapsulated magnetically active nuclei and to the NICS values at the center of the fullerenes (cf. Table 1). Thus, the different chemical shifts of nuclei encapsulated within the fullerene cages are easily explained.

The relative aromaticity of the fullerenes as estimated by the NICS in the cage center^{20,50} has been corroborated qualitatively by our model for the available fullerenes: C₆₀ (−11.3 ppm), C₆₀⁻⁶ (−64 ppm), C₇₀ (−25.9 ppm), and C₇₀⁻⁶ (−10.6 ppm). The aromaticity of the as yet unknown C₅₀ fullerene, however, was calculated (−10.7 ppm) to be smaller than previously reported.^{20,50} The same conclusions can be drawn from the magnetic susceptibilities of the five fullerenes studied; the corresponding values are given in Table 2. However, the TSNMR shieldings external to these fullerene cages proved to be even more interesting with respect to the (anti)aromaticity present.

External TSNMRS. TSNMRS external to the fullerenes C₅₀, C₆₀, C₆₀⁻⁶, C₇₀, and C₇₀⁻⁶ were visualized by an ICSS value of +0.1 ppm shielding (yellow) and −0.1 ppm deshielding (red) as portrayed in Figures 2–6 and proved to be highly informative.

C₆₀: Shielding above the hexagons and deshielding above the pentagons can be readily discerned (cf. Figure 2). In terms of aromaticity, this means that the six-membered rings are aromatic while the five-membered moieties are anti-aromatic for C₆₀, a result which is in complete agreement with both experimental measurements^{4,18,21,22} and other theoretical calculations.^{18,22} By employing ICSS values of ± 0.1 ppm for *in-plane* and *perpendicular-to-center* perspectives for aromatic ring systems as a simple means to estimate qualitatively the aromaticity of the system at hand,⁴⁹ distances in angstroms from the center of C₆₀ through the middle points of the hexagons (shielding, ICSS = +0.1 ppm) and of the pentagons (deshielding, ICSS = −0.1 ppm) have been determined and utilized to estimate qualitatively the local (anti)aromaticity above the surface of C₆₀. The corresponding values are given in Table 3. The method was also applied to the other fullerenes studied, and the results obtained are also given in Table 3 and are discussed in the following paragraphs (vide infra).

Besides the sign (shielding above six-membered ring moieties and deshielding above five-membered ring moieties), also the

(45) (a) Martin, N. H.; Allen, N. W., III; Moore, K. D.; Vo, L. J. *Mol. Struct. (THEOCHEM)* **1998**, *454*, 161. (b) Martin, N. H.; Allen, N. W., III; Moore, J. C. *J. Mol. Graph. Model.* **2000**, *18*, 242. (c) Martin, N. H.; Allen, N. W., III; Minga, E. K.; Ingrassia, S. T.; Brown, J. D. *Struct. Chem.* **1998**, *403*. (d) Martin, N. H.; Allen, N. W., III; Minga, E. K.; Ingrassia, S. T.; Brown, J. D. *Proceedings of ACS Symposium, Modeling NMR Chemical Shifts: Gaining Insight into Structure and Environment*; American Chemical Society: Washington, DC, 1999. (e) Martin, N. H.; Allen, N. W., III; Minga, E. K.; Ingrassia, S. T.; Brown, J. D. *Struct. Chem.* **1999**, *10*, 375. (f) Martin, N. H.; Allen, N. W., III; Ingrassia, S. T.; Brown, J. D.; Minga, E. K. *J. Mol. Graph. Model.* **2000**, *18*, 1. (g) Martin, N. H.; Nance, K. H. *J. Mol. Graph. Model.* **2002**, *21*, 51. (h) Martin, N. H.; Allen, N. W., III; Brown, J. D.; Kniec, D. M., Jr.; Vo, L. *J. Mol. Graph. Model.* **2003**, *22*, 127. (i) Martin, N. H.; Loveless, D. M.; Wade, D. C. *J. Mol. Graph. Model.* **2004**, *23*, 285.

(46) (a) Waugh, J. S.; Fessenden, R. W. *J. Am. Chem. Soc.* **1957**, *79*, 846. (b) Johnson, C. E.; Bovey, F. A. *J. Chem. Phys.* **1958**, *29*, 1012. (c) Jonathan, N.; Gordon, S.; Dailey, B. P. *J. Chem. Phys.* **1962**, *36*, 2443. (d) Barfield, M.; Grant, D. M.; Ikenberry, D. *J. Am. Chem. Soc.* **1975**, *97*, 6956. (e) Agarwal, A.; Barnes, J. A.; Fletcher, J. L.; McGlinchey, M. J.; Saver, B. G. *Can. J. Chem.* **1977**, *55*, 2575. (f) Haigh, C. W.; Mallion, R. B. *Progress in NMR Spectroscopy*; Pergamon Press, Ltd.: New York, 1980; Vol. 13, p 303.

(47) Haigh, C. W.; Mallion, R. B. *Mol. Phys.* **1971**, *22*, 955.

(48) (a) Haigh, C. W.; Mallion, R. B. *Org. Magn. Reson.* **1972**, *4*, 203. (b) Dailey, B. P. *J. Chem. Phys.* **1964**, *41*, 2304.

(49) Kleinpeter, E.; Klod, S.; Koch, A. *J. Mol. Struct. (THEOCHEM)* **2007**, *811*, 45.

(50) Lu, X.; Chen, Z.; Thiel, W.; Schleyer, P. v. R.; Huang, R.; Zheng, L. *J. Am. Chem. Soc.* **2004**, *126*, 14871.

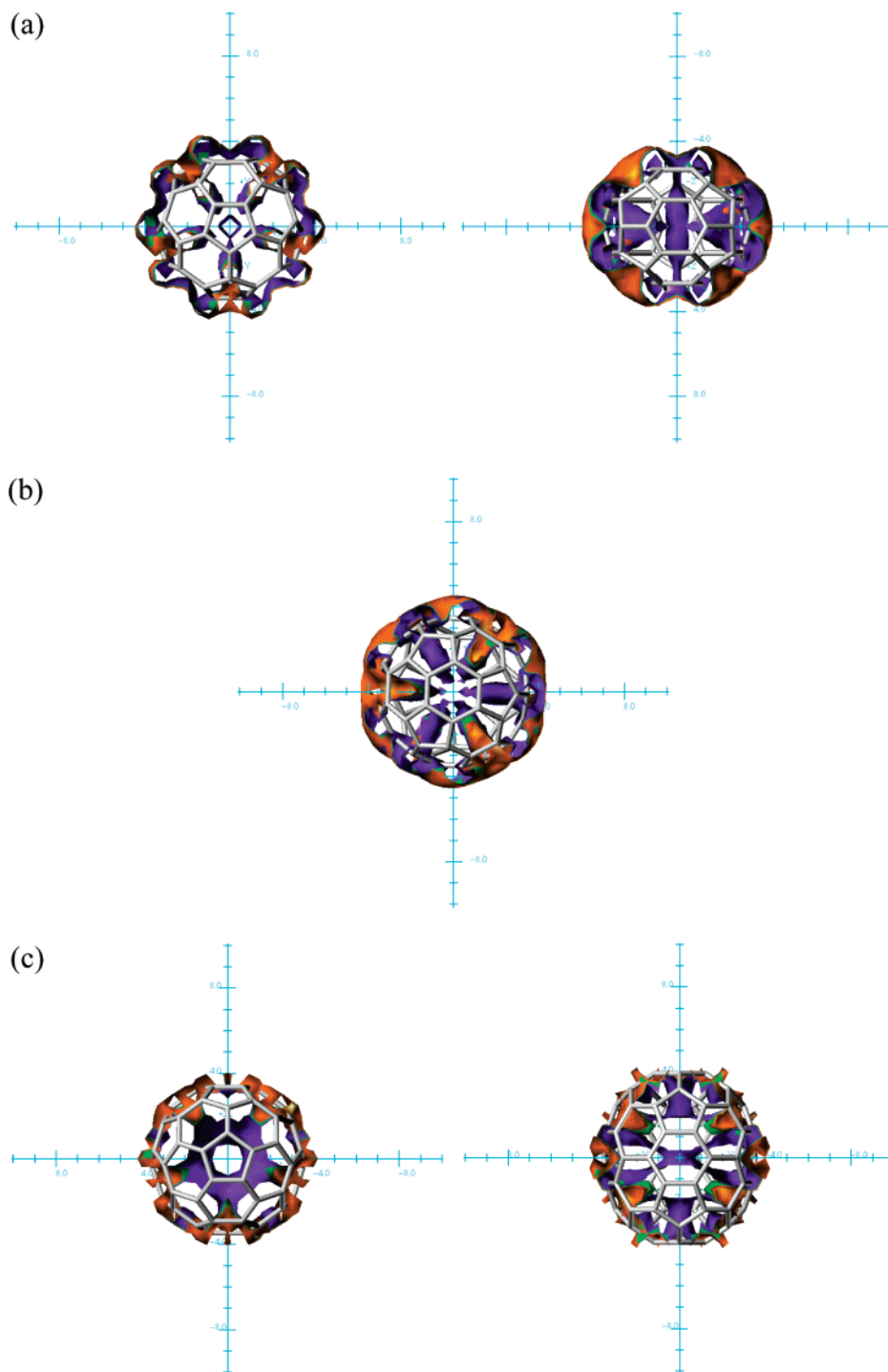


FIGURE 1. Visualization of the endohedral TSNMRS of C_{50} : (a) ICSS: orange 9.0, green 10.2, purple 10.72. C_{60} : (b) ICSS: orange 10.5, green 11.0, purple 11.25. C_{70} : (c) ICSS: orange 24.0, green 25.0, purple 26.0.

intensities of local aromaticity or anti-aromaticity were able to be estimated for C_{60} . The hexagons proved to be less aromatic than the pentagons are anti-aromatic, also in agreement with previous theoretical calculations.^{18,22} Cyclopentadiene, calculated by our procedure,²⁴ shows a combined anisotropic effect of the conjugated C=C double bonds which proves cyclopentadiene to be neither aromatic nor anti-aromatic.⁵² Thus, the deshielding above the five-membered ring moieties of C_{60} is the result of the local anti-aromaticity of this fullerene.

C_{60}^{-6} : External TSNMRS for the fullerene anion C_{60}^{-6} are visualized as ICSS of ± 0.1 ppm in Figure 3: it can be seen

that the anti-aromatic character of the five-membered ring moieties collapses and shielding above both five- and six-membered rings is found with approximately the same level of aromaticity (cf. Figure 3 and Table 3). Again, this is in complete agreement with experimental observations. Aromaticity is strongly increased (NICS at the center -64.4 ppm and magnetic

(51) Haddon, R. C.; Schneemeyer, L. F.; Waszczak, J. V.; Glarum, S. H.; Tycko, R.; Dabbagh, G.; Kortan, A. R.; Muller, A. J.; Muijsce, A. M.; Rosseinsky, M. J.; Zahurak, S. M.; Mikhija, A. V.; Thiel, F. A.; Raghavachari, K.; Cockayne, E.; Elser, V. *Nature* **1991**, *350*, 46.

(52) Stanger, A. *Chem.—Eur. J.* **2006**, *12*, 2745.

TABLE 1. NICS Values, Theoretical, and Experimental Chemical Shifts of Magnetically Active Nuclei Encapsulated within Various Fullerenes

fullerene	NICS/ppm	calculated δ /ppm	experimental δ /ppm
C ₅₀	-40.3 ⁵⁰ -36.6 ²⁰	He@C ₅₀ (-30.3) ^{16a}	-
		He@C ₅₀ (-38.0) ^{16a}	-
C ₆₀	-11.2 ²⁰	He@C ₆₀ (-9.0) ¹⁵	He@C ₆₀ (-6.0) ^{1a}
		H ₂ @C ₆₀ (-8.0) ^{6a}	H ₂ @C ₆₀ (-5.41) ^{a,6}
		Li ⁺ @C ₆₀ (-14.5) ¹⁵	Xe@C ₆₀ (-8.89) ⁵
		H ₂ O@C ₆₀ (-11.59) ^{a,9}	H ₂ O@C ₆₀ (-11.40) ^{a,9}
C ₆₀ ⁻⁶	-64.4 ²⁰	He@C ₆₀ ⁻⁶ (-58.3) ¹⁵	He@C ₆₀ ⁻⁶ (-48.7) ^{1e}
C ₇₀	-29.3 ²⁰	He@C ₇₀ (-24.3) ¹⁵	He@C ₇₀ (-28.8) ^{1a,c}
			He ₂ @C ₇₀ (deshielded by 0.014 ppm from He@C ₇₀) ²
			He@C ₇₀ ⁻⁶ (8.2) ³
			He ₂ @C ₇₀ ⁻⁶ (shielded by 0.15 ppm from He@C ₇₀ ⁻⁶) ³
C ₇₀ ⁻⁶	-10.6 ²⁰		

^a Obtained from open fullerenes.^{6,9}

TABLE 2. Magnetic Susceptibility (χ) of the Fullerenes Studied

molecule	χ (cgs·ppm)
C ₅₀	-233
C ₆₀	-292 (-260) ^a
C ₆₀ ⁻⁶	-929
C ₇₀	-706 (-550) ^a
C ₇₀ ⁻⁶	-245

^a Experimental values.⁵¹

susceptibility $\chi = -929$ cgs·ppm; cf. Tables 1 and 2), and clearly the additional electrons are concentrated on the C₆₀⁻⁶ pentagons transforming their anti-aromaticity into aromaticity. With respect to the distances from the center of C₆₀⁻⁶, the hexagons remain slightly more aromatic than the pentagons (cf. Table 3).

C₇₀: Similar conclusions concerning the external (anti-)aromaticity of C₇₀ can be drawn from the corresponding TSNMRS visualized with an ICSS of ± 0.1 ppm in Figure 4. As for C₆₀, shielding is observed above the six-membered ring moieties and deshielding above the five-membered rings. However, due to the ellipsoidal geometry of C₇₀, this fullerene contains different five- and six-membered ring moieties with distinct deshielding TSNMRS values (cf. Figure 4 and Table 3). With respect to C₆₀, shielding above the two different six-membered ring moieties is altered with a strengthening of the shielding above the hexagons in *equatorial* positions leading to an extended shielding belt (ICSS of +0.1 ppm > 10 Å) concomitant with a reduction of the shielding above the others, that is, a decrease in aromaticity for these latter segments. For the five-membered rings, stronger deshielding is observed and the difference between the *equatorial* and *apical* pentagons is exacerbated; the change above the *apical* pentagons is particularly dramatic (cf. Figure 4 and Table 3).

As the main result of this study, strengthened local aromaticity above *equatorial* hexagons and dropping aromaticity above the others, as well as extremely increased anti-aromaticity above the *apical* pentagons and moderate increased anti-aromaticity above the remaining pentagons, can be concluded.

Wilson and Lu^{21f} compared the ¹H chemical shift of the N-Me protons in the three isomers of the *N*-methylazomethine ylide of C₇₀ (cf. Table 5) and found them to be deshielded from typical aliphatic pyrrolidines ($\delta = 2.74, 2.60, \text{ and } 2.51$ ppm cf. to 2.32 ppm in *N*-methylpyrrolidine). The closer they are positioned to the *apical* regions of C₇₀, the more deshielded they are.^{21f} This experimental result is in complete agreement

with our TSNMRS (cf. Figure 4) wherein anti-aromaticity above the *apical* pentagon proved to be much stronger than that above the pentagons near the C₇₀ belt.

C₇₀⁻⁶: With respect to C₇₀, the six additional π -electrons present in C₇₀⁻⁶ confer changes to the (anti)aromaticity above the hexagons and pentagons both in size and direction (cf. Figure 5); these electrons are located mainly in the five-membered rings converting them from paratropic to diatropic rings.^{21k} Hereby, the former shielding belt of hexagons becomes anti-aromatic (i.e., deshielding results), including the hexagons in the second row close to the poles. The pentagons on the other hand induce shielding; that is, they are aromatic in nature, especially at the poles (*apical* positions). The newly created aromaticity due to the concentration of the six extra π -electrons is extraordinarily strong, all this in excellent agreement with experiment.^{21j,k} For the methylene-substituted product C₇₁H₂⁻⁶, two derivatives have been found with distinct CH₂ ¹H chemical shift differences. At the poles ($\Delta\delta > 2.5$ ppm), this reversal of aromaticity is strongest and only of modest size in the second row ($\Delta\delta = 1.26$ ppm), both in complete agreement with our calculated TSNMRS values. Thus, both the (anti)aromaticity and the corresponding NMR spectroscopic ring current effects above the hexagons and pentagons have been definitively corroborated by means of the calculated TSNMRS and visualized by ICSS of ± 0.1 ppm.

C₅₀: Isolation of the first stable C₅₀ fullerene derivative (C₅₀-Cl₁₀)⁵³ and the experimental⁵³ and theoretical⁵⁰ reporting of its spectroscopic and electronic properties have been made. Therefore, we also applied our method to this smallest carbon cage lacking three directly or subsequently fused pentagons. This fullerene, which is expected to be much more stable than other small fullerenes,⁵⁴ can exist as one of either two isomers for which ab initio calculations predicted the D₃ isomer to be the global energy minimum, and therefore, only this isomer was further considered.^{50,55,56} The ICSS of ± 0.1 ppm reveals the external (de)shielding surfaces for this structure (cf. Figure 6), and there are some interesting implications. First and foremost, deshielding is again observed above the *equatorial* pentagons at about the same level as that obtained for C₆₀ (cf. Table 3), while shielding is observed above the *equatorial* hexagons, but at a stronger intensity than in C₆₀. As a novelty, the hexagons around the *apical* pentagons form a common shielding surface. Therefore, it can be concluded that local aromaticity in C₅₀ has been found in the *apical* regions, while both aromaticity and anti-aromaticity are present in the *equatorial* regions.

To rationalize this unexpected result of apical C₅₀ aromaticity, we compared the pentagon geometries in C₅₀, C₆₀, and C₇₀; the results are collected in Table 4. Fullerenes are spherical molecules with some pyramidalization of their carbon atoms, and the pyramidalization angle θ_p ⁵⁷ was found to correlate well with the ¹³C chemical shifts of fullerenes^{58,59} and was used to rationalize the spread of chemical shifts in the molecules;⁶⁰ thus,

(53) Xie, S.-Y.; Gao, F.; Lu, X.; Huang, R.-B.; Wang, C.-R.; Zhang, X.; Liu, M.-L.; Deng, S.-L.; Zheng, L.-S. *Science* **2004**, *304*, 699.

(54) Kroto, H. W. *Nature* **1987**, *329*, 529.

(55) Wang, D.-L.; Shen, H.-T.; Gu, H.-M.; Zhai, Y.-C. *J. Mol. Struct. (THEOCHEM)* **2006**, *776*, 47.

(56) Diaz-Tendero, S.; Alcamí, M.; Martín, F. *Chem. Phys. Lett.* **2005**, *407*, 153.

(57) Haddon, R. C.; Scott, L. T. *Pure Appl. Chem.* **1986**, *58*, 137.

(58) Schulman, J. M.; Disch, R. L. *J. Comput. Chem.* **1998**, *19*, 189.

(59) Ferrer, S. M.; Molina, J. M. *J. Comput. Chem.* **1999**, *20*, 1412.

(60) Meier, M. S.; Spielmann, H. P.; Bergosh, R. G.; Haddon, R. C. *J. Am. Chem. Soc.* **2002**, *124*, 8090.

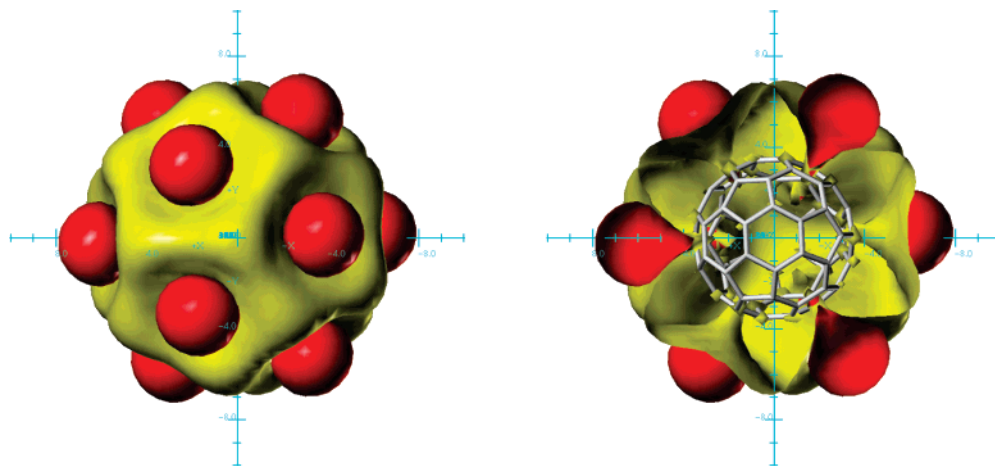


FIGURE 2. Visualization of the TSNMRS of C_{60} (ICSS: yellow 0.1 ppm shielding, red -0.1 ppm deshielding).

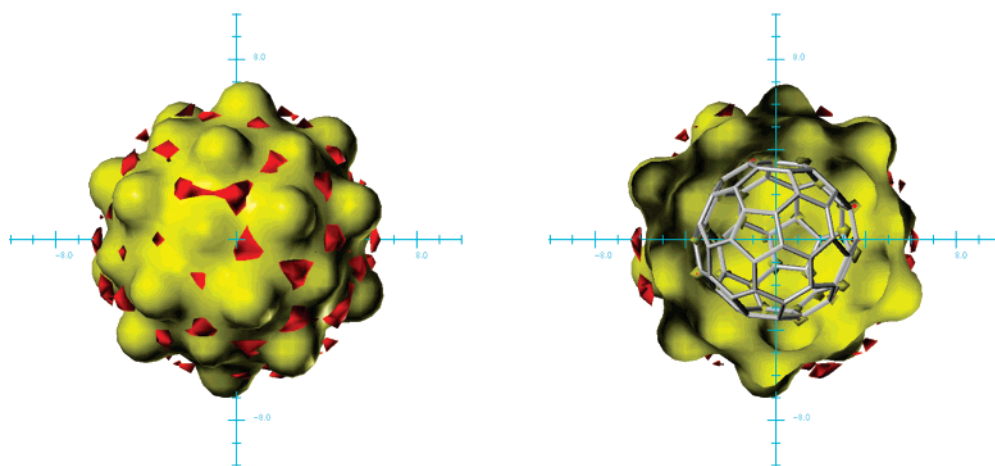


FIGURE 3. Visualization of the TSNMRS of C_{60}^{-6} (ICSS: yellow 0.1 ppm shielding, red -0.1 ppm deshielding).

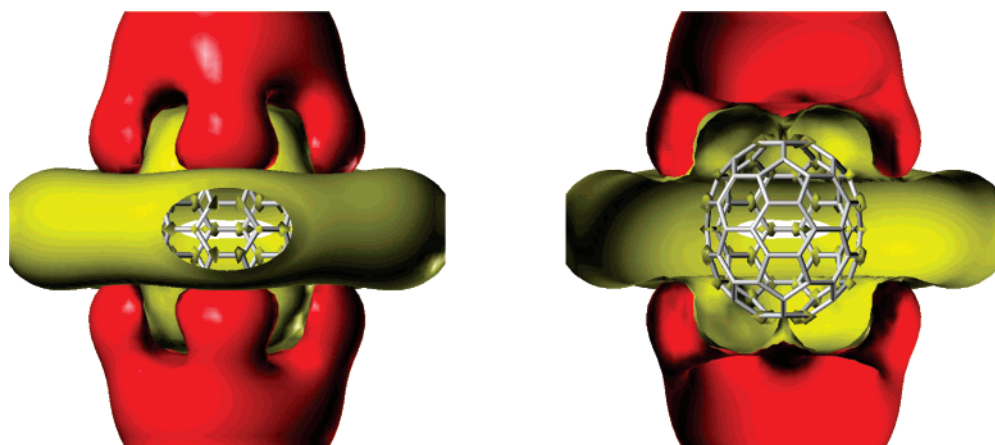


FIGURE 4. Visualization of the TSNMRS of C_{70} (ICSS: yellow 0.1 ppm shielding, red -0.1 ppm deshielding).

the sum of the endohedral angles in the pentagons is reduced compared with a fully planar structure (360°). In this respect, the identical structures of the pentagons in C_{60} serve as a reference (348°). In both C_{50} and C_{70} , which have different five-membered ring moieties, this angle parameter is decreased to 345.5° (C_{50}) and 347.3° (C_{70}) for the pentagons of stronger anti-aromaticity but increased to 349.78° (C_{50}) and 348.53° (C_{70}) for the pentagons of lower anti-aromaticity. In the case of C_{50} ,

the *apical* pentagon even contributes aromaticity to the surrounding six-membered ring moieties.

As an underlying cause for these observations, we have two explanations: (i) Changes in geometry lead to changes in π -electron distribution, probably in the localized ring currents, and thereby vary both the local aromaticity and the chemical shifts;⁶⁰ in the case of pentagons, this result changes the local anti-aromaticity. (ii) Alternatively, the relative positions of

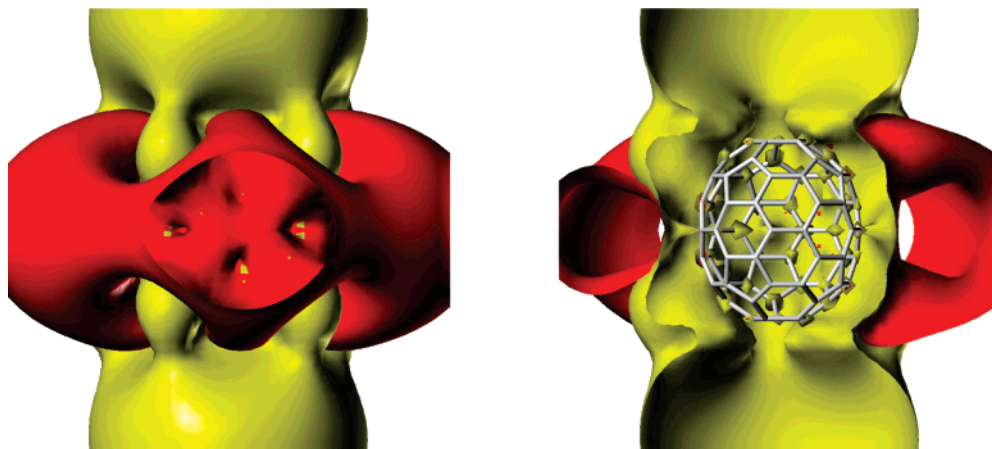


FIGURE 5. Visualization of the TSNMRS of C_{70}^{-6} (ICSS: yellow 0.1 ppm shielding, red -0.1 ppm deshielding).

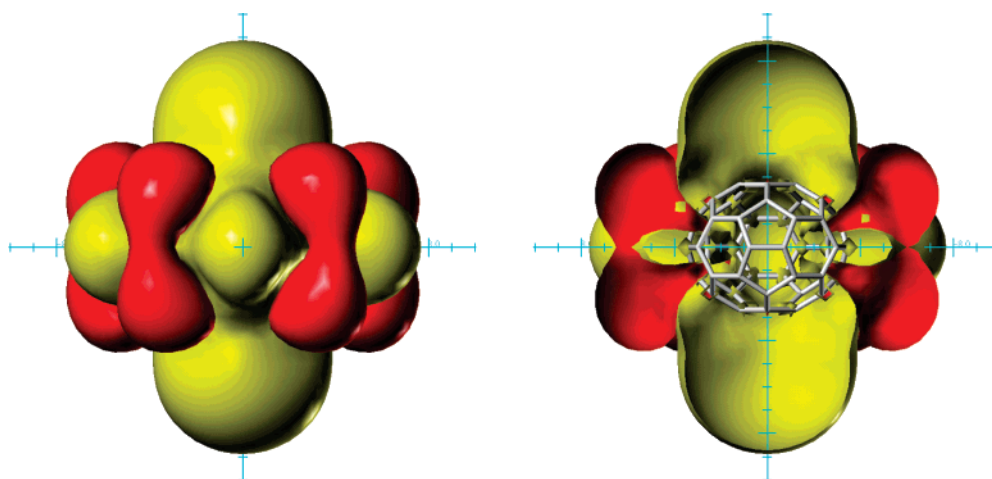


FIGURE 6. Visualization of the TSNMRS of C_{50} (ICSS: yellow 0.1 ppm shielding, red -0.1 ppm deshielding).

TABLE 3. ICSS Distances at ± 0.1 ppm from the Center of the Fullerenes through the Middle Points of the Five- and Six-Membered Ring Moieties, Respectively

fullerene	ICSS (\AA) of -0.1 ppm (deshielding) above	ICSS (\AA) of $+0.1$ ppm (shielding) above
	five-membered ring moieties	six-membered ring moieties
C_{60}	7.90	7.13
C_{60}^{-6}	6.50	7.10
C_{70}	13.50, ^a 7.85	11.20, ^b 6.20
C_{70}^{-6}	8.0 ^c (15.5 ^d)	12.1 ^e
C_{50}	7.88, 8.85 ^c	7.98 ^b

^a Apical. ^b Equatorial. ^c Shielding. ^d Apical but shielding. ^e Deshielding.

TABLE 4. Endohedral Angles in Pentagons in Various Fullerenes

angle	planar	C_{60}	C_{70} (a)	C_{70} (b)	C_{50} (a)	C_{50} (b)
angle 1	126	120.0	119.65	120.08	120.89	120.19
angle 2	126	120.0	119.65	119.94	120.89	118.48
angle 3	108	108.0	108.0	108.51	108.0	106.78
sum	360	348.0	347.30	348.53	349.78	345.45

pentagons and hexagons to each other *and* their geometries could lead to changes in the (anti)aromaticity of both pentagons and hexagons. If the aromatic hexagons are positioned beside weakly anti-aromatic pentagons—wherein only the sum of shielding and deshielding is calculated—this leads to overlap of the two with shielding dominating over the deshielding of the five-membered ring moieties (e.g., the *apical* regions of C_{50}). On the other hand,



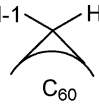
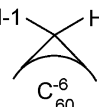
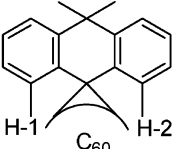
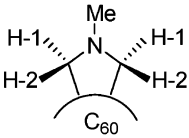
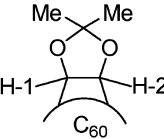
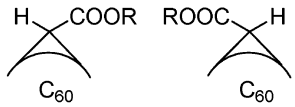
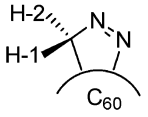
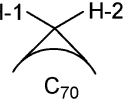
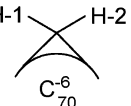
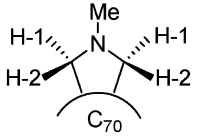
in the neighborhood of the shielding regions of weakly aromatic hexagons to strongly anti-aromatic pentagons, this can lead to overall deshielding covering the shielding regions of the aromatic moieties (e.g., at the *apical* regions of C_{70}). Each of these two explanations are reasonable in their own right, though it is likely that in reality the changes in the (de)shielding [(anti)-aromaticity] of the external regions of the C_{50} , C_{60} , and C_{70} series of fullerenes results from a combination of the two.

Calculation of the ^1H Chemical Shifts in Fullerene Derivatives Applied as Probes for Local (Anti)Aromaticity.

The ^1H chemical shifts of suitably substituted fullerene derivatives were employed to provide qualitative information about the localized (anti)aromaticity;^{18,22} relevant data published so far are collected in Table 5. Depending on the position of the protons above the carbon cages, they are either shielded when positioned above the aromatic moieties or deshielded when positioned above the anti-aromatic moieties. When the two protons are both positioned above hexagons, no chemical shift differentiation was observed, in line with former assessments.

There is one dramatic change in C_{60}^{-6} (this molecule was also calculated by the addition of six electrons to $C_{61}\text{H}_2$ without geometrical relaxation, and the chemical shifts obtained are given in Table 5): the proton above the pentagon is no longer deshielded as in $C_{61}\text{H}_2$, contrastingly, it is strongly shielded. This can be interpreted as being consistent with the pivotal

TABLE 5. ^1H Chemical Shifts of Protons above the Carbon Cages of Fullerene Derivatives

Fullerene derivative  = 	^1H chemical shifts δ/ppm					
	H-1	experimental H-2	$\Delta\delta$	H-1	calculated H-2	$\Delta\delta$
 C_{60}	3.93 ^{21b} 2.87 ^{21b}	3.93 ^{21b} 6.35 ^{21a}	0 3.48	3.08 2.80	3.08 6.40	0 3.60
 C_{60}^{-6}	2.33 ^{21l} 2.74 ^{21b}	2.33 ^{21l} 1.34 ^{21h}	0 -1.40	- 2.50	- 2.10	- -0.60
 C_{60}	7.21 ^{21d}	7.87 ^{21d}	0.66	-	-	-
 C_{60}	4.40 ^{21c}	-	-	-	-	-
 C_{60}	6.67 ^{21d}	6.77 ^{21d}	2.10	-	-	-
 C_{60}	- -	- -	3.45 ^{21e} (3.47) ^{21e}	-	-	-
 C_{60}	2.87 ^{21a}	6.35 ^{21a}	3.48	-	-	-
 C_{70}	2.95 ^{21b} 2.78 ^{21g} 2.88 ^{21k}	6.52 ^{21b} 5.23 ^{21g} 2.88 ^{21k}	3.57 2.45 0	2.85 2.57 2.37	5.65 5.29 2.37	2.80 2.72 0
 C_{70}^{-6}	2.27 ^{21b} 2.34 ^{21k} 2.77 ^{21l}	-0.255 ^{21k} 3.6 ^{21k} 2.77 ^{21l}	2.525 1.26 0	3.4 - -	-0.7 - -	4.1 - -
 C_{70}	3.43 ⁴⁾ 2.60, 3.58 and 3.92 ^{21f} 2.60 ^{21f} , 3.43 ^{21f} 2.51 ^{21f} , 2.27 ^{21f} 3.99 ^{21f}	3.68 ⁴⁾ 3.68 ^{21f} 2.31 ^{21f} 4.04 ^{21f}	0.25 0 0.25 0.04 0.05	- - - - -	- - - - -	- - - - -

N-Me all downfield ($\delta = 2.74, 2.60$ and 2.51 ppm, resp.), due to ring current effect on the surface of the C_{70} cage

TABLE 6. Comparison of the NICS in C₆₀ and C₇₀ with Experimental Chemical Shifts of the CH₂ Protons in C₆₁H₂ and C₇₁H₂

compound	NICS of C ₆₀ and C ₇₀ at the corresponding positions of potential CH ₂ protons in C ₆₁ H ₂ and C ₇₁ H ₂ , respectively			Experimental chemical shifts of CH ₂ protons		
	above pentagon	above hexagon	Δδ	above pentagon	above hexagon	Δδ
	C ₆₀	-0.96	0.68	1.64	6.35	2.78
C ₆₀ ⁻⁶	0.59	1.09	0.5	1.35	2.74	1.4
C ₇₀	-1.80	0.66	2.46	6.52	2.95	3.57
C ₇₀ ⁻⁶	-0.63	0.42	1.05	5.23	2.78	2.45
	5.05 ^a	0.90 ^a	4.15 ^a	-0.255 ^a	2.27 ^a	2.525 ^a
	1.44 ^b	-0.23 ^b	1.67 ^b	3.6 ^b	2.34 ^b	1.26 ^b

^a Apical pentagon included. ^b Second type of pentagons included.

change in localized aromaticity upon reduction.²² The proton chemical shifts of the methylene protons in the fullerene derivatives, positioned above one pentagon and one hexagon, were also calculated employing the GIAO perturbation method (included in Table 5). In the case of C₆₀ and C₇₀, the agreement between experiment and theory is reasonable. Not only are the shielding/deshielding effects of the hexagon and pentagon moieties, respectively, reproduced, but, in particular, the strong shielding above the C₆₀⁻⁶ pentagons is excellently calculated.

Thus, our calculations are congruent: the correct reproduction of the chemical shifts of protons proximal to the fullerene surfaces impressively corroborates the correctness of structures which are the basis for the TSNMRS and ICSS obtained.

Local Ring Current Effect of Fullerenes on Proximal Protons in Fullerene Derivatives. Next, the ICSS values of C₆₀ and C₇₀ were incorporated into the structures of C₆₁H₂ and C₇₁H₂, respectively (and also the corresponding TSNMRS of C₆₀⁻⁶ and C₇₀⁻⁶ into the structures of C₆₁H₂⁻⁶ and C₇₁H₂⁻⁶, respectively), and the NICS values at the positions of the two CH₂ protons in C₆₁H₂ and C₇₁H₂, respectively, were determined subject to the TSNMRS values of C₆₀ and C₇₀, respectively (the same procedure was applied to estimate the NICS of the CH₂ protons in C₆₁H₂⁻⁶ and C₇₁H₂⁻⁶, subject to the spacial NICS of C₆₀⁻⁶ and C₇₀⁻⁶). The ensuing results are contained in Table 6. Both experimental and theoretically calculated chemical shift differences, Δδ, of the CH₂ protons are larger than the NICS values; however, (i) the correct (de)shielding above the hexagons and pentagons are predicted, (ii) the shielding above the hexagons in C₆₀ and C₇₀ remains about the same as deshielding occurs above pentagons, and (iii) the Δδ of the CH₂ protons in C₇₀ increases with respect to C₆₀. In addition, (iv) the same effects in C₆₀⁻⁶ and C₇₀⁻⁶ are reversed: the CH₂ proton above the pentagon is actually more shielded than the corresponding proton above the hexagon, in complete agreement with experiment. Actually, the shielding of 5.05 ppm above the C₇₀⁻⁶ apical pentagons is overestimated (Δδ_{calc} = 4.15 ppm, Δδ_{exp} = 2.525 ppm), but the experimental chemical shift of the corresponding proton (δ = -0.255 ppm) even to the right of TMS corroborates the correctness of the results as obtained by our model.

Conclusions

Experimental chemical shifts of both enclosed magnetically active nuclei and external protons proximal to the fullerene surface excellently corroborate *through-space NMR shieldings (TSNMRS), calculated as spatial NICS, to exactly reproduce*

the local aromaticity endohedrally and on the surface of fullerenes: (i) Both endohedral (Figure 1) and external (anti-)aromaticity (Figures 2–6) of the fullerene carbon cages of C₅₀, C₆₀, C₆₀⁻⁶, C₇₀, and C₇₀⁻⁶ could be visualized. (ii) The shielding (aromaticity) inside the carbon cages proves to be not homogeneous but heterogeneous; the position of magnetically active nuclei in the cavities determines their chemical shift subject to spherical (anti)aromaticity. (iii) Differences in (anti)aromaticity of five- and six-membered ring moieties of the fullerenes C₅₀, C₆₀, C₆₀⁻⁶, C₇₀, and C₇₀⁻⁶ were determined quantitatively by the isochemical shielding surfaces (ICSS) at ±0.1 ppm; the results are in excellent agreement with magnetic susceptibilities and theoretical calculations. (iv) Experimental ¹H chemical shifts in fullerene derivatives are in excellent agreement with ab initio calculated chemical shifts and in good agreement with TSNMRS values at the certain positions; thus, ring current effects (aromaticity/antiaromaticity) strongly but not exclusively determine the ¹H chemical shifts of external protons in fullerene derivatives.

Experimental Section

Ab initio calculations were performed on SGI Octane and SGI Origin 2000 workstations or a Linux cluster using the *Gaussian03* program package.⁶¹ Geometry optimizations were performed at the B3LYP/6-31G* level of theory⁶² without restrictions. The chemical shieldings in the surroundings of the molecules were calculated based on the NICS concept²⁵ whereby the molecule was placed in the center of a grid of ghost atoms ranging from -10.0 to +10.0 Å in all three dimensions with a step width of 0.5 Å, resulting in a cube of 68 921 ghost atoms. The chemical shielding calculations were performed using the GIAO^{26,27} method at the HF/6-31G*//B3LYP/6-31G* level of theory. Since GIAO is a coupled HF method that uses gauge-independent atomic orbitals for the calculation of shielding values, it can be used for the calculation of NICS values. When X-ray structures were available from the Cambridge crystallographic data base,⁶³ they were employed as starting structures for the ab initio calculations; otherwise starting structures were generated by SYBYL modeling software.²⁸ From the GIAO calculations, the coordinates and isotropic shielding values of the ghost atoms were extracted. After transformation of the tabulated chemical shieldings into a SYBYL²⁸ contour file, the TSNMRS of the molecules were visualized as ICSS, providing a 3-D view on the spatial extension, sign, and scope of the anisotropic effects at

(61) Frisch, M. J.; Trucks, G. W.; Schlegel, H. B.; Scuseria, G. E.; Robb, M. A.; Cheeseman, J. R.; Montgomery, J. A., Jr.; Vreven, T.; Kudin, K. N.; Burant, J. C.; Millam, J. M.; Iyengar, S. S.; Tomasi, J.; Barone, V.; Mennucci, B.; Cossi, M.; Scalmani, G.; Rega, N.; Petersson, G. A.; Nakatsuji, H.; Hada, M.; Ehara, M.; Toyota, K.; Fukuda, R.; Hasegawa, J.; Ishida, M.; Nakajima, T.; Honda, Y.; Kitao, O.; Nakai, H.; Klene, M.; Li, X.; Knox, J. E.; Hratchian, H. P.; Cross, J. B.; Adamo, C.; Jaramillo, J.; Gomperts, R.; Stratmann, R. E.; Yazyev, O.; Austin, A. J.; Cammi, R.; Pomelli, C.; Ochterski, J. W.; Ayala, P. Y.; Morokuma, K.; Voth, G. A.; Salvador, P.; Dannenberg, J. J.; Zakrzewski, V. G.; Dapprich, S.; Daniels, A. D.; Strain, M. C.; Farkas, O.; Malick, D. K.; Rabuck, A. D.; Raghavachari, K.; Foresman, J. B.; Ortiz, J. V.; Cui, Q.; Baboul, A. G.; Clifford, S.; Cioslowski, J.; Stefanov, B. B.; Liu, G.; Liashenko, A.; Piskorz, P.; Komaromi, I.; Martin, R. L.; Fox, D. J.; Keith, T.; Al-Laham, M. A.; Peng, C. Y.; Nanayakkara, A.; Challacombe, M.; Gill, P. M. W.; Johnson, B.; Chen, W.; Wong, M. W.; Gonzalez, C.; Pople, J. A. *Gaussian03*, revision C.02; Gaussian, Inc.: Wallingford, CT, 2004.

(62) Hehre, W. J.; Radom, L.; Schleyer, P. v. R.; Pople, J. A. *Ab initio Molecular Orbital Theory*; Wiley & Sons: New York, 1986.

(63) Cambridge Crystallographic Data Centre, 12 Union Road, Cambridge, UK, 2004: (a) Zhou, O.; Fischer, J. E.; Coustel, N.; Kycia, S.; Zhu, Q.; McGhie, A. R.; Romanow, W. J.; McCauley, J. P., Jr.; Smith, A. B., III; Cox, D. E. *Nature* **1991**, *351*, 462. (b) Soldatov, A. V.; Roth, G.; Dzyabchenko, A.; Johnels, D.; Lebedkin, S.; Meingast, C.; Sundquist, B.; Haluska, M.; Kuzmany, H. *Science* **2001**, *293*, 680.

each point in space. Magnetic susceptibilities of the fullerenes studied were calculated by the continuous set of gauge transformations (CSGT) method.⁶⁴⁻⁶⁶

(64) Keith, T. A.; Bader, R. F. W. *Chem. Phys. Lett.* **1992**, *194*, 1.

(65) Keith, T. A.; Bader, R. F. W. *Chem. Phys. Lett.* **1993**, *210*, 233.

(66) Cheeseman, J. R.; Frisch, M. J.; Trucks, G. W.; Keith, T. A. *J. Chem. Phys.* **1996**, *104*, 5497.

Acknowledgment. Dr. Karel D. Klika is thanked for correction of the language.

Supporting Information Available: Coordinates and absolute energies at the B3LYP/6-31G* level of theory for the fullerenes studied. This material is available free of charge via the Internet at <http://pubs.acs.org>.

JO702316H